CHARACTERIZATION OF A TWO-WAY COUPLING APPROACH FOR THE SIMULATION OF FLUID FLOWS UNDER CRYOGENIC CONDITIONS

Rúben Meireles, Leandro Magalhães*, André Silva, Jorge Barata
LAETA - Aeronautics and Astronautics Research Center,
University of Beira Interior,
6201-001 Covilhã,
Portugal,
E-mail: leandro.magalhaes@ubi.pt

ABSTRACT

Ice formation at lifting surfaces and engine intakes is a significant issue affecting regular aircraft operation. The icing on a wing's leading edge perturbs the airflow around the wing, contributing to a decrease in lift and increasing drag. A step towards the understanding of droplet dynamics under cryogenics is made in the present work. An in-house developed tool is used to study the impact of droplet diameter and air humidity ratio in free-falling water droplets' flow dynamics. The 3D Navier-Stokes equations are solved in a RANS-based two-way coupling model, which considers that the carrier fluid properties are modified by the presence of a dispersed phase, accounting for mass exchange momentum and energy between them. A Lagrangian/Eulerian formulation is employed to model each of the considered phases. The results obtained are compared with a one-way modeling approach and experimental data to infer the interacting phases' effect in the overall process dynamics. In this way, it is possible to conclude that for high humidity content, this interaction is predominant and, consequently, needs to be taken into consideration. However, for low humidity ratios, the one-way coupling is a sufficient approximation to the experimental data.

NOMENCLATURE

A	[$\mathrm{m^2}$]	Surface area
c	[$\mathrm{J\,kg^{-1}\,K^{-1}}$]	Specific heat capacity
d	[m]	Droplet diameter
e	[−]	Emissivity
h_h	[$\mathrm{W\,m^{-2}\,K^{-1}}$]	Convective heat transfer coefficient
h_m	[$\mathrm{m\,s^{-1}}$]	Convective mass transfer coefficient
L	[$\mathrm{J\,kg^{-1}}$]	Specific latent heat
q	[$\mathrm{kg\,s^{-3}}$]	Heat flux per unit area
T	[K]	Temperature
t	[s]	Time
U	[$\mathrm{m\,s^{-1}}$]	Velocity
V	[$\mathrm{m^3}$]	Volume
x, y, z	[m]	Cartesian axis direction

Special characters

ϵ	[$\mathrm{m^2\,s^{-3}}$]	Dissipation of turbulence kinetic energy
k	[$\mathrm{m^2\,s^{-2}}$]	Turbulence kinetic energy
ρ	[$\mathrm{kg\,m^{-3}}$]	Specific mass
σ	[$5.6704 \times 10^{-8}\,\mathrm{W\,m^{-2}\,K^{-4}}$]	Stefan–Boltzmann constant

Subscripts

∞	Far-field region
d	Particle
g	Gas
h	Convective heat transfer
m	Convective mass transfer
p	Isobaric
ph	Phase change
r	Thermal radiation
wv	Water vapor

INTRODUCTION

As sophisticated as technology may be, climacteric conditions remain a factor of paramount importance in aircraft operations. The impingement of water droplets in the form of freezing rain, freezing drizzle, or snow particulates and its accumulation on aircraft lifting surfaces and engine intakes are a barrier to safe aircraft operation. Supercooled water droplets represent a metastable phase, where the principle of minimal energy is only observed for a global analysis, making these types of droplets susceptible to be disturbed for an array of atmospheric conditions. For instance, according to Cao et al. [1], the total drag of an aircraft can increase between 100 % and 300 % depending on the ice regime.

Through the years, several reports were prepared on the subject of icing-related incidents/accidents. In 2015, Green [2], published the Icemaster database and an analysis of aircraft aerodynamic icing-related accidents and incidents. In this report, a period from 1982 to 2010 is considered for aircraft operation in the United States. Further information was compiled by Jones et al. [3] on a subsonic aircraft safety icing study. Dillingham [4], organized the icing and winter weather-related incident reports, for large commercial aircraft, by category of the incident, between 1998 and 2007. These studies unveiled the actual danger of ice accretion and alerted for the disregard and lack of research in this area.

In this sense, the cooling and freezing of water droplets have received more attention from researchers in recent years. Zarling [5] performed a theoretical and numerical analysis of a system of droplets in free fall to evaluate the variations in the humidity ratio, enthalpy, and temperature of the surrounding air and the droplets. On the other hand, Hindmarsh et al. [6] performed an experimental analysis for a suspended freezing water droplet's temperature transition and developed a numerical model that predicted a four-stage supercooling process. In contrast, in 2011, Tanner [7] performed a droplet freezing and solidification study in which a four-stage freezing model was presented.

More recently, Meng and Zhang [8] carried out a study that considered the dynamic propagation of ice-water phase front in a supercooled water droplet. In his research, a three-dimensional theoretical model was proposed accounting for crystallization kinetics during heat transfer. In the same year, Akhtar et al. [9] developed and validated a semi-analytical framework for the freezing of droplets, considering heterogeneous nucleation and non-linear interface kinetics. Myers et al. [10] addressed a Stefan problem with variable thermophysical properties and phase change temperature for a water droplet on a standard one-dimensional problem.

Apart from the aeronautical industry, different areas such as food, refrigeration, and wind energy can better understand the freezing and cooling phenomena. Advances in this field would enable to increase the overall performance and efficiency of different systems, mitigate structural and mechanical failures, enlarge the lifetime of devices, reduce economic damage via the loss of millions of euros in services and products, and, ultimately, prevent the loss of human lives.

The proposed manuscript aims to serve as a stepping stone for developing an in-house numerical solver capable of predicting ice accretion and impact on lifting surfaces. As a result, a numerical investigation is performed in the present work to predict the cooling of free-falling water droplets.

The remaining of the manuscript is organized as follows: a brief explanation of the underlying physical models used is made in the following section, followed by a summary of the Eulerian/Lagrangian coupling between the considered phases. The physical description leads to the description of the numerical algorithm, for which experimental conditions available in the literature are imposed as initial and boundary conditions. Representative results of the physical phenomena at play are selected for presentation to provide insight into the intricacies of flows at such conditions, for which conclusions are drawn, taking into account the advantages and limitations of the proposed methodology.

PHYSICAL AND MATHEMATICAL MODELS - COOLING PROCESS

Assuming that the particle integrates a thermodynamic system, a simple heat balance model is used to obtain the temperature profile for airborne droplets' cooling process in a cold atmosphere. The rate at which the temperature of the droplet changes with time is given by Eq. (1). The subscript d denotes the particle properties, $c_{p,d}$ is the specific heat capacity at constant pressure, ρ_d the specific mass, T_d the temperature, V_d the volume, and A_d the surface area. The parameters q_h, q_m, and q_r denote the heat fluxes (per unit area) due to convective heat and mass transfer, and thermal radiation. Additionally, $T_{g,\infty}$ is the temperature of the ambient gas in the far-field region, h_h the convective heat transfer coefficient, L_{ph} the specific latent heat of phase change, h_m the convective mass transfer coefficient, e the emissivity and σ the Stefan–Boltzmann constant of radiation.

Concerning the convention used for the heat transfer between the droplet and the surrounding environment, considering a water droplet in a free fall surrounded by a humid air gas stream and the heat exchange inherent to the process, the heat fluxes due to the convective heat transfer and thermal radiation have an outward flux to the surrounding environment. However, since we are in a cooling process, the heat flux due to convective mass transfer has an inwards movement. Since the temperature differences between the droplet and the far-field region of the gas are significant, a diffusive-convective region appears around the droplet. In this region, the temperature is given by combining the droplet and gas temperatures, being described as a reference temperature.

$$\rho_d V_d c_{p,d} \frac{dT_d}{dt} = \\ -A_d \left(\overbrace{h_h \left(T_d - T_{g\infty}\right)}^{q_h} + \overbrace{L_{ph} h_m \left(\rho_{wv} - \rho_g\right)}^{q_m} + \overbrace{e\sigma \left(T_d^4 - T_g^4\right)}^{q_r} \right) \tag{1}$$

Nevertheless, even when considering a simple balance between the droplet and the surrounding environment, it is necessary to consider the transport processes' impact in the interior of the particle. Yao and Schrock [11] proposed three models to represent these phenomena: complete mixing model, non-mixing model, and mixing model. The simplest model assumes that the droplet's internal motion is so vigorous that complete mixing is achieved. This was the assumption considered when formulating Eq. (1).

To obtain the convective heat and mass transfer coefficients' values, it is usual to use correlations based on empirical data. Ranz and Marshall [12; 13] developed a correlation for the case of steady-state heat transfer of solid spheres. This correlation is commonly known as the Ranz-Marshall classical formulation (RM) and is represented by Eq. (2) resorting to the Nusselt (Nu) and Sherwood (Sh) numbers, based on droplet Reynolds (Re), Schmidt (Sc), and Prandtl (Pr).

$$\begin{cases} \mathrm{Nu_d} = 2 + 0.6\mathrm{Re_d}^{1/2}\mathrm{Pr_d}^{1/3} \\ \mathrm{Sh_d} = 2 + 0.6\mathrm{Re_d}^{1/2}\mathrm{Sc_d}^{1/3} \end{cases} \tag{2}$$

However, Yao and Schrock [11] concluded that for certain conditions, the vibrations and deformations of the falling droplets have an impact on heat and mass transfer coefficients and, for that reason, have to be accounted for. Therefore, those authors presented a Ranz-Marshall corrected formulation (RMcf), accounting for those effects since the first formulation considers a complete mixing model. This new formulation results in multiplying the corrective factor presented in Eq. (3) on Eq. (2). In this way, the corrected formulation represents a mixing model assumption. In the equation, z stands for the distance traveled by the droplet.

$$C.F = 25\left(\frac{z}{d}\right)^{-0.7} \tag{3}$$

Therefore, in this work, the droplets' convective effects are accounted for using those two correlations. The corrected formulations are valid for droplets with diameters between 3 and 6 mm and a ratio of distance to diameter between 10 and 600.

TWO-WAY COUPLING - CONTINUOUS AND DISPERSED PHASES

When dealing with low mass-loading ratio particles, the influence of these particles on the surrounding environment is small and, for that reason, it is not necessary to account for that interaction. Therefore, from a mathematical perspective, this phenomenon can be approached by a one-way coupling methodology. However, when the particles' mass-loading ratio increases, it is necessary to consider the mutual influence between those particles and the surrounding environment. This approach is well-detailed in Rodrigues [14]. To model this phenomenon mathematically, a Lagrangian frame is used to follow the particles' trajectory, with an Eulerian frame employed for solving the surrounding environment.

The Reynolds-averaged conservation equations for mass, momentum, and energy are considered for incompressible flow. In the dispersed phase, the droplets are treated as discrete objects, and their motion is tracked as they move through the flow field. To obtain their position and velocity, the trajectories of representative samples are obtained by solving the particle momentum equation through the Eulerian fluid velocity field, which is acquired by solving the averaged Navier-Stokes equations. One significant parameter of these equations that has to be accounted for is the particle relaxation time. It is a consequence of examining particles' motion inside a carrier fluid and depends on the particle inertia and its free-fall velocity.

The time step selected to obtain the trajectory equations' discrete form (position and velocity over time) is determined considering an eddy-particle interaction time. This parameter is defined as the minimum value between the turbulent eddy lifetime time scale and the eddy transit time, considering that the fluctuating velocity associated with a particular eddy is constant over the interaction time. The coupling between the two-phases is accomplished using an iterative procedure to obtain a converged solution. The system of equations is closed with the κ–ϵ turbulence model of Launder and Spalding [15].

NUMERICAL ALGORITHM

To consider the exchange of mass, momentum, and energy between the two phases in dilute flows, both phases have to be coupled. The implemented procedure follows the presented sequence to obtain a converged solution for both phases.

1. Definition of initial conditions and initialization of source terms.
2. Mesh generation to represent the computational domain of the problem.
3. Definition of the droplets, or spray, characteristics.
4. Initialization of the continuous phase calculated disregarding the source terms of the dispersed phase (source terms of the discrete phase equal to zero), obtaining a converged solution for the gas flow field.
5. Dispersed phase initialization. In this phase, the particles are tracked through the flow field, and the values for the source terms are obtained.
6. Recalculation of the continuous phase considering the new source terms of the dispersed phase to obtain a converged solution for the gas flow field.
7. Compare the solutions for the continuous phase with the new particle source terms by determining the residues and verify if they are smaller than the convergence criteria.
8. Repeat steps five, six, and seven until the overall convergence is obtained. Otherwise, calculate one last time

the dispersed phase with the values obtained from the particle source terms of the dispersed phase.

For pressure-velocity coupling, the velocities are evaluated at the cell's edge in a staggered grid configuration. For this case, the discretization scheme selected was the QUICK scheme of Leonard [16]. The SIMPLE algorithm reported in Patankar and Spalding [17], which derives an equation for pressure from the momentum and continuity equations based on a guess-and-correct procedure, was used for the pressure-velocity coupling. The Tridiagonal Matrix Algorithm (TDMA), suggested by Thomas [18], was used to solve the resulting system.

INITIAL CONDITIONS AND BOUNDARY CONDITIONS

To compare the experimental and numerical results obtained by Yao and Schrock [11] and Magalhães [19], a computational domain that resembles the experimental setup is considered. The setup consists of a plastic column of a squared base with 0.170 m of edge, 3 m of height, and a droplet generator. The droplet generator is set on the center of the upper face and, an air stream is injected downwards from the upper face into the lower face with a velocity of 0.03 $\mathrm{m\,s^{-1}}$. Figure 1 represents a three-dimensional scheme configuration of the computational domain used.

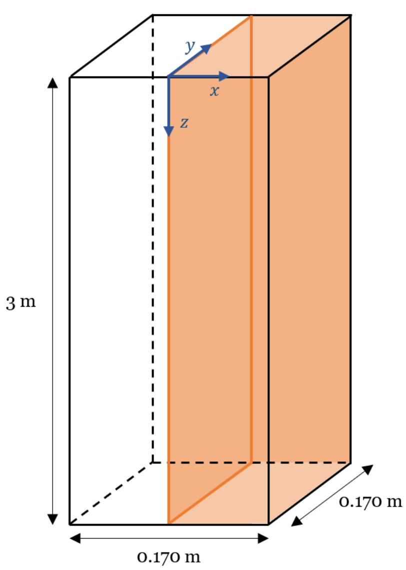

Figure 1: Three-dimensional configuration of the computational domain.

Besides, to speed up the numerical calculations, considering the existence of a symmetry plane for $x = 0$, only half of the column was considered, represented by the section in orange in Figure 1. Therefore, the numerical results which correspond to the full extent of the column are obtained by symmetry. The Cartesian reference frame has its origin on the upper face and is represented in blue. Therefore, four different Boundary Conditions are considered: both an inlet and outlet, a symmetry plane, and three solid walls representing the column's sides.

RESULTS

To ensure that the numerical results do not depend on the discretized space, a grid independence study was performed using three levels of refinement with 9660 (coarse mesh), 19200 (fine mesh), and 38000 (finest mesh) points in a structured orthogonal mesh of rectangular elements. The fine mesh is used to maintain grid independence.

Figure 2, 3 and 4 correspond, respectively, to the temperature profile of a single water droplet falling through the air for three distinct air humidity ratios, 0.29, 0.36, and 1.00. Attending the experimental data gathered by Yao and Schrock [11] different diameters appear for distinct air humidity ratios.

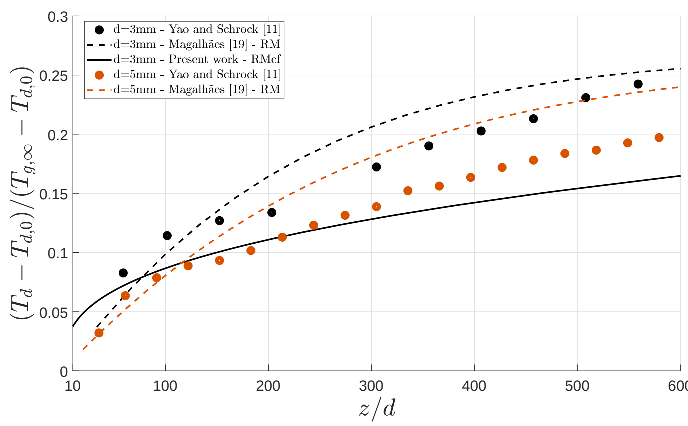

Figure 2: Variation on a single water droplet temperature, falling through the air, with an air humidity ratio of 0.29 and a variable droplet diameter.

Analyzing Figure 2 and considering the results for a diameter of 3 mm, the numerical data from the two-way coupling model have good correspondence with experimental data up to a falling height of 80 diameters. From that point on, the one-way coupling methodology predicts the phenomenon in proximity to the experimental data up to a falling distance of 150 diameters and then from 500 diameters up to the end of the domain. The cooling phenomenon is overestimated between those distances, but these results still outperform the ones obtained by using the two-way coupling methodology. For this case, the Ranz-Marshall classical formulation corresponds to a better approximation to the experimental data.

Considering a droplet diameter of 5 mm, the one-way coupling methodology follows the experimental data temperature tendency. Up to a falling distance of 120 diameters, this model precisely follows the data gathered by Yao and Schrock [11]. From that point on, the one-way coupling model still shows proximity with the experimental data but overestimates the cooling phenomenon. For this diameter, the complete mixing model assumption is the one that is near the experimental values.

Observing Figure 3, for a droplet diameter of 3 mm the two-way couple model shows close agreement with experimental data up to a falling height of 310 diameters. From that point on, the numerical results presented by Magalhães [19] predict the experimental data more accurately.

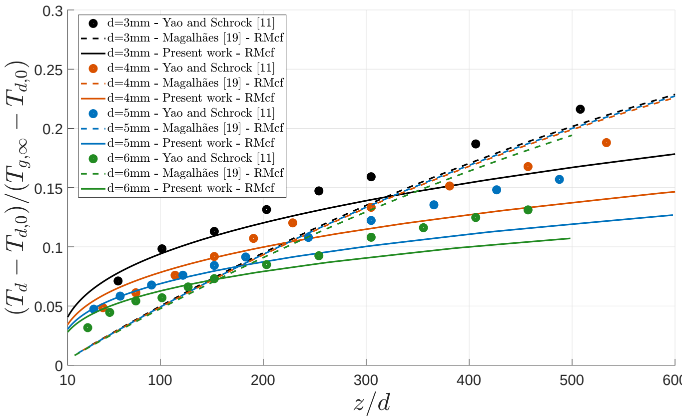

Figure 3: Variation on a single water droplet temperature, falling through the air, with an air humidity ratio of 0.36 and a variable droplet diameter.

When examining a diameter of 4 mm, a similar situation occurs but, this time, the falling height, at the change between the two models occurs, is smaller. Up to a falling height of 230 diameters, the two-way coupling model is the one that represents the cooling phenomenon more accurately. From that point on is the one-way coupling model that shows close agreement with experimental data.

For a diameter of 5 mm the two-way coupling model predicts more accurately the experimental results up to a falling height of 190 diameters and, from that point on is the numerical data gathered by Magalhães [19] which closely represents the experimental study performed by Yao and Schrock [11].

Finally, for a diameter of 6 mm, the two-way coupling model is the one that shows the closest agreement with experimental data for the entire domain.

Additionally to what was previously said, it is seen that the mixing model assumption, based on the Ranz-Marshall corrected formulation assumption, is the one that predicts the cooling phenomenon more precisely for any given droplet diameter.

Examining Figure 4, for a droplet diameter of 3 mm the complete mixing model has a close agreement with the experimental data up to a falling height of 510 diameters. From that point on, the deformations and vibrations are predominant since the Ranz-Marshall corrected formulation simulates more accurately the cooling phenomenon.

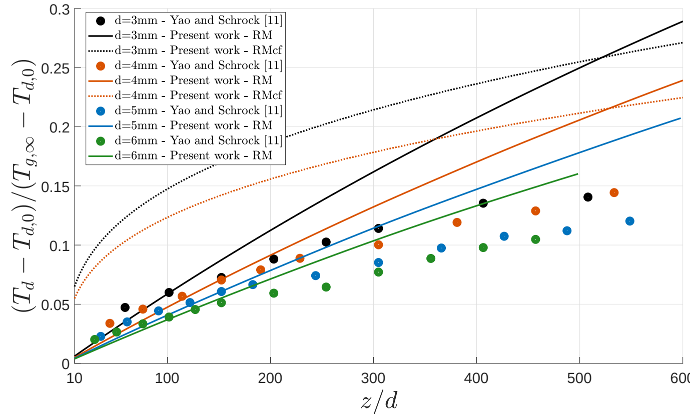

Figure 4: Variation on a single water droplet temperature, falling through the air, with an air humidity ratio of 1.00 and a variable droplet diameter.

Considering a diameter of 4 mm, a similar situation occurs. Up to a falling height of 550 diameters, the complete mixing model assumption shows better results compared to the mixing model assumption. However, from that point on, it becomes clear that the vibrations and deformations become predominant.

Finally, for the diameters of 5 mm and 6 mm, the complete mixing model is the one that shows the best agreement with experimental data, and therefore, it is concluded that for these two diameters, the cooling phenomenon vibrations and deformations can be neglected.

Also, it is clear that for all diameters, the two-way coupling methodology is the one that shows better results when compared with the experimental data, suggesting that the mutual interference between the droplet and the surrounding environment is predominant for this air humidity ratio.

CONCLUSIONS

An in-house developed tool is used to study the impact of droplet diameter and air humidity ratio in the flow dynamics considering a RANS-based two-way coupling model to solve the 3D Navier-Stokes equations and a Lagrangian/Eulerian formulation for the distinct phases.

Numerical predictions resorting to the two-way coupling model are near experimental data, for any diameter, when considering high humidity ratios. However, these predictions failed to replicate the data obtained experimentally for lower humidity ratios, where the one-way coupling represents the best match. Therefore, it is suitable to interpret that, for high humidity content, the mutual interaction between the droplet and the surrounding environment becomes predominant and needs to be accounted for. When considering low humidity content, this mutual interaction can be neglected since the one-way coupling resembles the experimental data closely. The transition criterion is set at intermediate humidity ratios, connected to increasing droplet diameter.

Moreover, the complete mixing model is an acceptable assumption when considering low or high humidity ratios (0.29 and 1.00) since the results obtained when resorting to the Ranz-Marshall classical formulation predict the cooling phenomenon, for any diameter, more accurately indicating a steady-state regime for these conditions. On the other hand, when considering an intermediate level of humidity (0.36), the complete mixing model could not predict the phenomenon accurately enough since the Ranz-Marshall corrected formulation simulated the phenomenon more accurately, suggesting that the mixing model assumption is acceptable for these conditions.

ACKNOWLEDGMENT

The present work was performed under the scope of activities at the Aeronautics and Astronautics Research Center (AEROG) of the Laboratório Associado em Energia, Transportes e Aeronáutica (LAETA), and was supported by the Fundação para a Ciência e Tecnologia (Project No. UIDB/50022/2020).

REFERENCES

[1] Cao, Y., Tan, W., and Wu, Z. Aircraft icing: An ongoing threat to aviation safety. *Aerospace Science and Technology*, Vol. 75, 2018, pp. 353–385.

[2] Green, S. D. DOT/FAA/TC-14/44 - The ice-master database and an analysis of aircraft aerodynamic icing accidents and incidents. Federal Aviation Administration, William J. Hughes Technical Center Aviation Research Division, June 2015.

[3] Jones, S. M., Reveley, M. S., Evans, J. K., and Barrientos, F. A. NASA/TM-2008–215107 - Subsonic aircraft safety icing study. NASA - National Aeronautics and Space Administration, January 2008.

[4] Dillingham, G. L. GAO-10-441T - Aviation safety - Preliminary information on aircraft icing and winter operations. GAO - United States Government Accountability Office, February 2010.

[5] Zarling, J. P. Heat and mass transfer from freely falling drops at low temperatures. Tech. Rep. No. 18, Cold Regions Research and Engineering Laboratory, Hanover, New Hampshire, USA, August 1980.

[6] Hindmarsh, J. P., Russell, A. B., and Chen, X. D. Experimental and numerical analysis of the temperature transition of a suspended freezing water droplet. *International Journal of Heat and Mass Transfer*, Vol. 46, No. 7, 2003, pp. 1199–1213.

[7] Tanner, F. X. Droplet freezing and solidification. Springer U.S., Boston, MA, 2011, Chapter 16, pp. 327–338.

[8] Meng, Z., and Zhang, P. Dynamic propagation of ice-water phase front in a supercooled water droplet. *International Journal of Heat and Mass Transfer*, Vol. 152, 2020, p. 119468.

[9] Akhtar, S., Xu, M., and Sasmito, A. P. Development and validation of a semi-analytical framework for droplet freezing with heterogeneous nucleation and non-linear interface kinetics. *International Journal of Heat and Mass Transfer*, Vol. 166, 2020, p. 120734.

[10] Myers, T. G., Hennessy, M. G., and Calvo-Schwarzwälder, M. The Stefan problem with variable thermophysical properties and phase change temperature. *International Journal of Heat and Mass Transfer*, Vol. 149, 2020, p. 118975.

[11] Yao, S.-C., and Schrock, V. E. Heat and mass transfer from freely falling drops. *American Society of Mechanical Engineers*, Vol. 98, No. 1, 1976, pp. 120–126.

[12] Ranz, W. E., and Marshall, W. R. Evaporation from drops: Part 1. *Chemical Engineering Progress*, Vol. 48, No. 3, 1952, pp. 141–146.

[13] Ranz, W. E., and Marshall, W. R. Evaporation from drops: Part 2. *Chemical Engineering Progress*, Vol. 48, No. 4, 1952, pp. 173–180.

[14] Rodrigues, C. M. G. Modelling of a biofuel spray wall impingement. PhD Thesis, University of Beira Interior, Covilhã, Portugal, October 2015.

[15] Launder, B. E., and Spalding, D. B. The numerical computation of turbulent flows. *Computer Methods in Applied Mechanics and Engineering*, Vol. 3, No. 2, 1974, pp. 269–289.

[16] Leonard, B. P. A stable and accurate convective modelling procedure based on quadratic upstream interpolation. *Computer Methods in Applied Mechanics and Engineering*, Vol. 19, No. 1, 1979, pp. 59–98.

[17] Patankar, S. V., and Spalding, D. B. A calculation procedure for heat, mass and momentum transfer in three-dimensional parabolic flows. *International Journal of Heat and Mass Transfer*, Vol. 15, No. 10, 1972, pp. 1787–1806.

[18] Thomas, L. H. Elliptic problems in linear differential equations over a network. Watson Sci. Comput. Lab Report, Columbia University, New York, 1949.

[19] Magalhães, L. B. Numerical study of freezing water droplets. Master's Thesis, University of Beira Interior, Covilhã, Portugal, May 2016.